One-dimensional Brownian-motion model for transport measurements in high-temperature superconductors

Ch. Goupil, T. Aouaroun, D. Thopart, J. F. Hamet, and Ch. Simon
CRISMAT ISMRA Centre National de la Recherche Scientifique, 6 Bd Mal Juin, 14050 Caen, France
(Received 18 April 1996; revised manuscript received 9 August 1996)

Using a one-dimensional model of Brownian motion of vortices over pinning wells, we derive a current-voltage equation assuming a distribution of the effective pinning length. The model describes linear and nonlinear regimes of the $E(J)$ curves in a single-particle description. Thermally activated flux flow and flux flow define the two limits of the dissipative process, respectively, at very low and high current. The pinning relief is described by pinning well depth and pinning well gradient, respectively, which can be checked by resistive and current-voltage measurements. The model is then applied to a $YBa_2Cu_3O_{7-\delta}$ thin film. It provides a phenomenological model of the dissipation induced by transport current. [S0163-1829(96)02045-0]

INTRODUCTION

The understanding of the pinning properties of high-temperature superconductors is of particular interest and was the subject of a great amount of work. Due to the important contribution of the disorder in such materials, only equilibrium states or established dissipative states correctly reflect the average macroscopical behavior of the superconductor. Following this way one can check for static properties like Bean critical current, or dynamic properties like dc or low-frequency transport measurements. In this paper we focus on the latter point considering current-voltage $[E(J)]$ and resistive $[\rho(T)]$ results.

Due to the high temperature and the smallness of the coherence length ξ, the dissipative mechanisms are mainly governed by thermally activated processes including fluctuation of vortices around an equilibrium position. Thus linear resistivity follows an Arrhenius law.[1,2] Vortices are pinned in wells of depth $U(T,B)$ and their escape rate is proportional to $\exp(-U/kT)$. In the presence of bulk current, the complete expression of the Kim-Anderson creep model is

$$E(J)=2Bv_0 l\ \exp\left(-\frac{U(T,B)}{kT}\right)\sinh\left(\frac{JBV_cR_P}{kT}\right), \quad (1)$$

where B is the flux density, v_0 is the characteristic escape rate, l is the mean jumping distance, V_c is the correlated vortex bundle, and R_p the pinning potential range. At sufficiently low current, Eq. (1) describes an Ohmic regime,[2,3]

$$E(J)=\frac{2B^2v_0 lJV_cR_P}{kT}\exp\left(-\frac{U(T,B)}{kT}\right), \quad (2)$$

which is the thermally activated flux-flow (TAFF) regime.

If one considers sufficiently high currents, the pinning wells become ineffective and dissipation occurs from a macroscopical motion of the entire vortex lattice. This flux-flow (FF) mechanism has been extensively studied during the 1960's.[4] The flow resistivity is proportional to the density of vortices (i.e., the flux density) and the inverse of the friction coefficient.

Thus

$$\rho_{\rm ff}=\frac{B\Phi_0}{\eta_{\rm ff}}. \quad (3)$$

One can note that creep and flow mechanisms have no connection in between, the creep process diverges when current is increasing. The single well hypothesis used in the Kim-Anderson model partly explain the dissipative results when only the average pinning energy is involved as in current-constant resistive measurements. On the other hand, this model fails when different pinning well effects are checked separately. Such phenomena is observed when measuring isothermal current-voltage characteristics. In this case, the current acts as a probe for the pinning well. While increasing, the current breaks down the efficiency of the well starting from the weakest to the strongest one. When the current reaches the value where no more wells are efficient then flux-flow occurs.

On the other side, at very low current, the TAFF reflects the breaking down of the weakest well. As we will show later, this regime can be unobservable due to the smallness of the corresponding dissipation level.

This simple description summarizes the natural connection which exists between TAFF and FF regimes. As done previously in other papers,[5–7] we also note the necessity of introducing a distribution of the well efficiencies for a correct description of $E(J)$ shape though it is not so crucial when considering isocurrent resistive measurements. Here we propose a one-dimensional analysis of the dissipative process assuming Brownian motion of noninteracting vortices in a distribution of wells.[9,7] This one-dimensional (1D) model does not consider thermal wandering of the vortex lines along the magnetic-field direction. This restricts the applicability of the model to thin films, or 3D samples in the low-temperature regime where line tension energy overcomes thermal wandering. This approach provides a description of the low-temperature regimes where thermal activation does not contribute much to vortices displacement. The current dependent force, acting on vortices, is then the main source of dissipation. Increased currents probe increasing pinning wells slope (and not necessary deepest wells) and then give an ''overview'' of the pinning relief of the sample

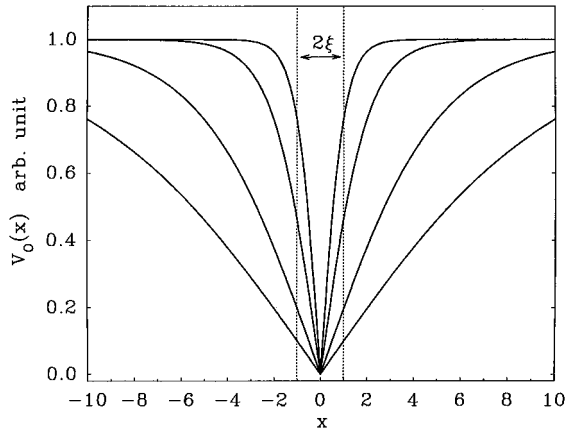

FIG. 1. Normalized pinning well shape for various values of the pinning well width $\delta/\xi=1$, 2, 5, 10.

in the form of a pinning well gradient distribution. When the main contribution to dissipation comes from thermal activation this approach is no longer valid and extracted distributions are meaningless. These observations restrict the validity of the model to regimes where collective effects can be neglected.

MODEL

In order to describe a typical well, we consider the condensation energy gain obtained when a vortex core stand on a defect where the superconducting order parameter $|\Psi|$ is depressed. If one assumes $|\Psi(r)|^2=|\Psi|_\infty^2 \tanh(r/\delta)$,[6,8] then in one dimension, the potential energy of the vortex in the well is given by

$$v(x)=V_0\left|\tanh\left(\frac{x}{\delta}\right)\right|, \tag{4}$$

where V_0 is the well depth and δ the effective width of the well (Fig. 1).

The Brownian motion of the vortices is expressed by the Langevin equation[9,7]

$$\frac{dv(x)}{dx}=F_c(J)-\eta_{\mathrm{ff}}a\dot{x}+L(t) \tag{5}$$

where a is the moving vortex length, η_{ff} is the friction coefficient, $dv(x)/dx$ is the restoring force, $F_c(J)=Ja\Phi_0$ is the current-dependent force acting on vortices, and $L(t)$ is a Gaussian white-noise function $[\langle L(t)\rangle=0, \langle L(t+\tau)L(t)\rangle=(2kT/\eta_{\mathrm{ff}})\delta(\tau)]$.

In order to solve Eq. (5), one can construct the associated Fokker-Planck equation and solve it using the Kramers's method.[10,9] The average velocity of the flux line is then given by

$$\langle\dot{x}\rangle=\frac{kT\{1-\exp[-F_c(J)\,\delta/kT]\}}{\eta_{\mathrm{ff}}a\int_0^\delta \exp[-F_c(J)x/kT]I_0[v(x)/kT]dx}, \tag{6}$$

where $I_0(u)$ is the zero-order modified Bessel function. $[I_0(u)\simeq 1+u^2/4$ for $u\to 0$, $I_0(u)\simeq\exp(u)/\sqrt{2\pi u}$ for $u\gg 1]$. Due to the motion of the line, the phase slippage of the order parameter induces an electrical field which allows current to

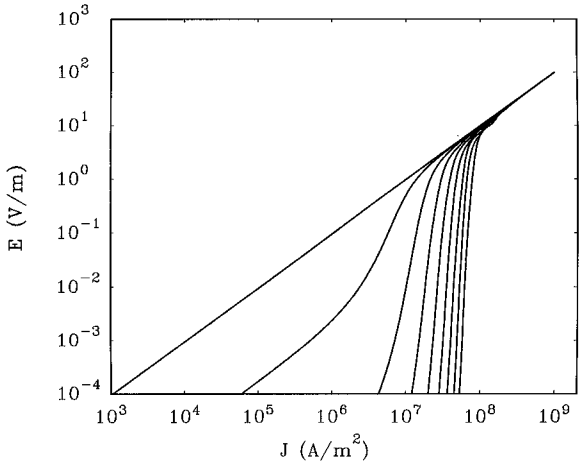

FIG. 2. Calculated $E(J,V_0,J_0)$ curves for various pinning well depth. From the left to the right: $V_0/kT=0$, 1, 4, 8, 12, 16, 20, 24, 28.

flow across the normal core of the vortex generating dissipation: $E=B\langle\dot{x}\rangle$. The moving vortices flow with constant velocity due to the compensation between current-induced force and viscous damping force. According to Eq. (3) we now get: $J\Phi_0=\eta_{\mathrm{ff}}\langle\dot{x}\rangle$ so,

$$E(J,V_0,\delta)=\frac{\eta_{\mathrm{ff}}\rho_{\mathrm{ff}}}{\Phi_0}\langle\dot{x}\rangle. \tag{7}$$

Thus

$$E(J,V_0,\delta)=\frac{\rho_{\mathrm{ff}}}{a\Phi_0}\frac{kT[1-\exp(-J/J_0)]}{\int_0^\delta \exp(-Jx/J_0\delta)I_0[V_0\tanh(x/\delta)/kT]dx} \tag{8}$$

with $J_0=kT/a\,\delta\Phi_0$, which is proportional to the pinning well gradient. We can easily rewrite Eq. (8) in the form

$$E(J,V_0,J_0)=\rho_{\mathrm{ff}}J\frac{[1-\exp(-J/J_0)]}{\int_0^{J/J_0}\exp(-x)I_0[V_0\tanh(J_0/Jx)/kT]dx}. \tag{9}$$

Only three parameters govern the dissipation process: the flux-flow resistivity ρ_{ff}, the well depth V_0 and the characteristic current J_0 which is related to the gradient of the pinning well.

We present in Fig. 2 the obtained $E(J,V_0,\delta)$ curve for various pinning well depths V_0. Equation (9) describes the dissipation mechanism when a pinning well of depth V_0 and gradient proportional to J_0 are assumed. Thus Eq. (9) can be expressed in the form

$$E(J,V_0,J_0)=\frac{\rho_{\mathrm{ff}}J}{F(J,V_0,J_0)} \tag{10}$$

with

$$F(J,V_0,J_0)=\frac{\int_0^{J/J_0}\exp(-x)I_0[V_0\tanh(J_0/Jx)/kT]dx}{[1-\exp(-J/J_0)]}, \tag{11}$$

which describes the energy required to overcome for depinning a vortex from a well. In other words, $[F(J,V_0,J_0)]^{-1}$ is equal to the vortex depinning probability. This expression fully incorporates both the thermal activation process and the current dependency contribution. Note that these two effects are clearly separated in the expression. This allows one to distinguish the thermally activated mechanism which probes the pinning well depth, from the current-dependent process which probes the gradient of the well more than its depth. In other words, in isothermal current-voltage measurements, *the increasing currents probe increasing well gradients*, while in isocurrent resistive measurements, *increasing temperatures probe increasing well depth*. Thus it is of great importance to separate the pinning energy $v(x)$ from the $F_c(J)$ work over the well slope. At very low currents, the main contribution to the dissipation is from the activated term and $F(J,V_0,J_0)$ reduces to $F(V_0)$ which does not depend on J and is approximately $F(V_0)\simeq I0[0.78(V_0/kT)]/[0.78(V_0/kT)/2+1]$.

PINNING WELL DISTRIBUTION

Let us consider now a system where pinning wells are distributed over their depth via V_0 and their width via J_0. In this paper we will only focus on isothermal current-voltage behavior. In this way and following the previous discussion, we consider only the pinning well gradient distribution. Assuming a distribution of parallel domains Eq. (10) becomes

$$E(J)=\rho_{\rm ff}J\left[\int_0^\infty \sigma(J_0)F(J,V_0,J_0)dJ_0\right]^{-1} \tag{12}$$

with the normalization condition $\int_0^\infty \sigma(J_0)dJ_0=1$. To conclude this part, let us say that distribution of activation energies can be studied in the same way, if very low current is assumed to avoid the perturbation of $\sigma(J_0)$ contribution to the extracted $\sigma(V_0)$ distribution.

FLUX FLOW AND THERMALLY ACTIVATED FLUX MOTION

Following Eq. (12), the current-voltage characteristics are described by an Arrhenius process over a distribution of pinning well efficient width. This result includes several previous analyses especially the Hagen-Griessen model[5] in which a distribution of pinning well energies induced a dissipative expression with TAFF and flux-flow processes involved.

If one considers high current $J/J_0\gg 1$, the pinning effect vanishes and thereby flux-flow dissipation occurs and expression (12) becomes Ohmic:

$$E(J)=\frac{\rho_{\rm ff}}{a\Phi_0}F_c(J)=\rho_{\rm ff}J. \tag{13}$$

Let us now consider low dissipation level, i.e., low-temperature, high pinning energy and very low currents, $J/J_0\ll 1$. Then expression (12) becomes

$$E(J)=\frac{\rho_{\rm ff}}{F(V_0)}J=\rho_{\rm Taff}J, \tag{14}$$

with $\rho_{\rm Taff}/\rho_{\rm ff}=[F(V_0)]^{-1}$. In other words, for a given temperature, $[F(V_0)]^{-1}$ represent the moving fraction of vortices. If we consider typical pinning energies, say $V_0=1250$ K, at $T=50$ K, then $\rho_{\rm Taff}/\rho_{\rm ff}\approx 2\times 10^{-9}$. Thus the TAFF regime in $E(J)$ measurement can be rejected to unobservable dissipation level. Here we want to point out that nonlinear behavior in the low dissipation regime observed in $E(J)$ curves does not prove that dissipation occurs with a nonlinear process at low current.[6,5] If we now consider a single well pinning process, then Eq. (9) simplifies to the creep model:

$$E(J)=\frac{\rho_{\rm ff}J_0}{F(V_0)}\left[\exp\left(\frac{J}{J_0}\right)-1\right]. \tag{15}$$

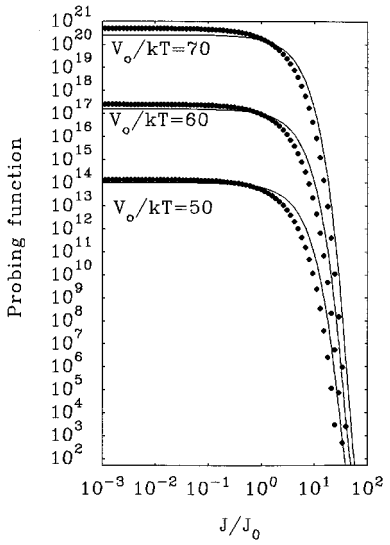

FIG. 3. Comparison of $F_{\rm app}(J,V_0,J_0)$ (black circle) and $F(J,V_0,J_0)$ (line) in reduced unity J/J_0 for three pinning well depth. Plot is given in log-log coordinates in order to compare to log-log $E(J)$ plots.

EXPERIMENTAL RESULTS

In order to test the validity of our assumptions, we recorded current-voltage measurements on a 500 Å YBaCuO thin film with $T_c=87$ K. The $\sigma(J_0)$ distributions were estimated considering the approximate probing function $F_{\rm app}(J,V_0,J_0)=1+(F(V_0)-1)\exp(-J/J_0)\simeq F(J,V_0,J_0)$ which summarizes the accumulated effects of V and J_0 to the depinning process. $F_{\rm app}(J,V_0,J_0)$ and $F(J,V_0,J_0)$ are plotted in Fig. 3. One can see that $F_{\rm app}(J,V_0,J_0)$ is not an exact description of $F(J,V_0,J_0)$ but gives sufficient confidence for data conversion over a wide range of current and voltage. We easily get from (12)

$$Z(J,V_0)=\frac{\rho_{\rm ff}J/E(J,V_0)-1}{F(V_0)-1}=\int_0^\infty \sigma(J_0)\exp\left(-\frac{J}{J_0}\right)dJ_0. \tag{16}$$

Note that $Z(J,V_0)$ is a very simple function to determine because only flux-flow and TAFF resistivity have to be estimated and by this the experimental treatments are easy to perform. The extracted results are summarized in Figs. 4–6, where both $E(J)$ curves and $\sigma(J_0)$ distributions are presented. All the distributions present a sharp maximum $J_{0_{\rm max}}$ which correspond to the pinning well length mostly encoun-

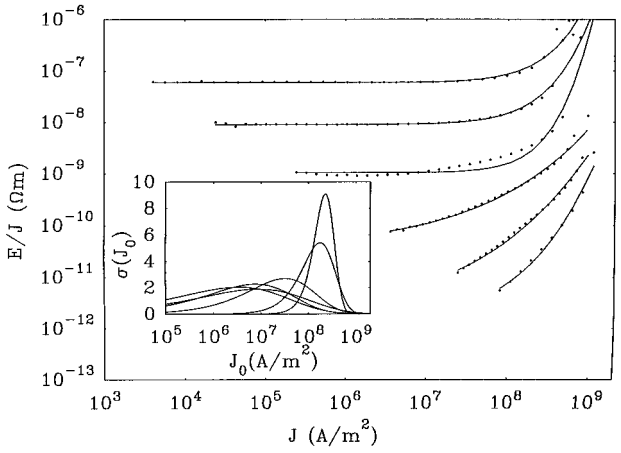

FIG. 4. E-J data for a YBaCuO thin film for an applied field of 0.1 T along the c axis, the black circles are experimental points and the line a phenomenological fit of the data (Ref. 5). The temperatures are given from the right to the left: 81.5, 82.1, 82.7, 83.4, 84.1, 84.9. Inset: extracted distribution of pinning well length. Vertical axis: arb.units.

tered. In this model, the pinning well range distribution was supposed to be temperature independent which is found to be not the case in the results. In order to highlight this point, we present in Fig. 7 the $J_{0_{\max}}$ versus temperature and magnetic field. The obtained curves show two parts separated by a characteristic temperature say T_{th}. Below T_{th}, $J_{0_{\max}}$ are temperature independent. This corresponds to the classical understanding of a distribution where $\sigma(J_0)$ describes the pinning relief, which is temperature independent, with a predominancy of a sharp pinning center of the order $J_{0_{\max}}^{-1}$. Above T_{th}, we observe a strong temperature dependency of $J_{0_{\max}}$. This behavior can be explained using the following image: due to thermal activation, the pinning relief is smoothed so the applied current which acts as a pinning

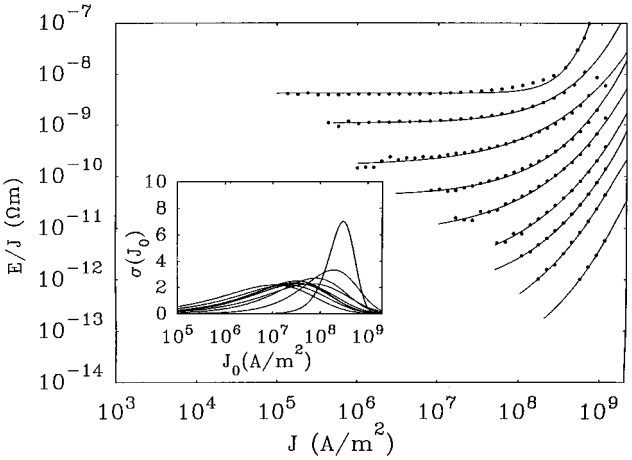

FIG. 5. E-J data for a YBaCuO thin film for an applied field of 1 T along the c axis, the black circles are experimental points and the line a phenomenological fit of the data (Ref. 5). The temperatures are given from the right to the left: 76.3, 77.3, 77.9, 78.4, 79, 79.5, 80.2, 80.9. Inset: extracted distribution of pinning well length. Vertical axis: arb.units.

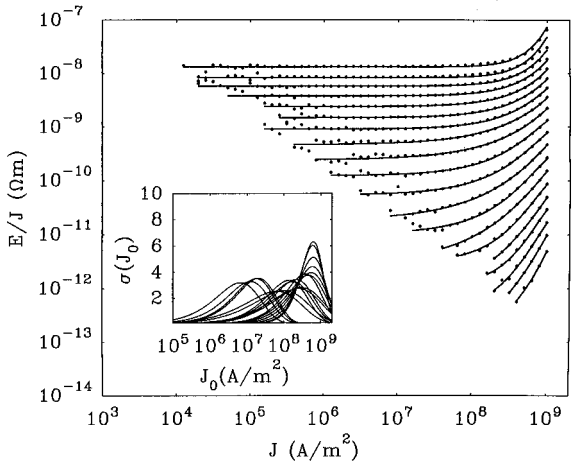

FIG. 6. E-J data for a YBaCuO thin film for an applied field of 5 T along the c axis, the black circles are experimental points and the line a phenomenological fit of the data (Ref. 5). The temperatures are given from the right to the left: 65.1, 65.7, 66.3, 67, 67.5, 68.2, 68.9, 69.6, 70.2, 70.8, 71.4, 71.9, 72.5, 72.9, 73.3, 73.7, 74.1, 74.5, 74.9, 75.4. Inset: extracted distribution of pinning well length. Vertical axis: arb.units.

gradient probe losses accuracy. The resulting $\sigma(J_0)$ image becomes fuzzy. In other words, the observed dissipation is mainly due to the work of the current-dependent force below T_{th} and thermally activated processes above. T_{th} appears to be the temperature above which the present model fails. As a consequence, the $\sigma(J_0)$ distribution is modified at high temperatures. This would require a new description of the pinning landscape where energy profiles would depend on the presence of neighborhood vortices, though we will not deal on this point in the present paper.

The $E(J)$ measurements (Figs. 4–6) present non-Ohmic regimes at low current for the lowest recorded temperatures. Such an observation is not proof that an Ohmic regime would not occur at lower currents. However, similar data have been often studied in the framework of the vortex-glass transition which predicts a crossover from Ohmic to non-Ohmic regimes. This has been the subject for a great amount

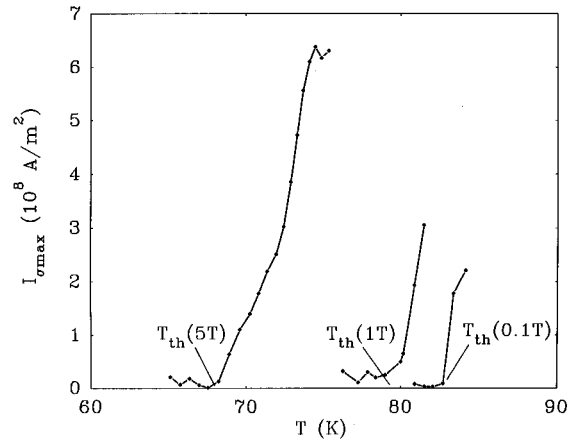

FIG. 7. Maxima of the distributions versus temperature. These maxima correspond to the mostly represented pinning well profiles. $T_{\text{th}}(B)$ indicate the independent to dependent temperature behavior of the maxima.

of work on various YBaCuO samples.[11–13] Using the same analysis we also found a vortex-glass transition temperature $T_g(B)$ and critical exponents $\nu=1.7$ and $z=5.5$ which are in good agreement with previous results. On the basis of such experimental results no conclusion can be derived in favor of one or the other model. We present this result in Fig. 8. It should be noticed that $T_{\rm th}(B)$ and $T_g(B)$ are roughly equal. This can be understood since $T_{\rm th}(B)$ represent the temperature above which the present model is no longer valid because dissipation is then mainly governed by thermal processes. Note that this description also fails for very low temperature and current regimes such as variable range hopping where resistivity presents nonlinear behavior.[16]

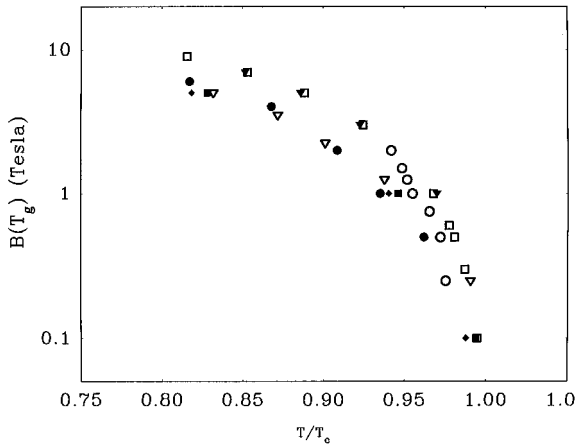

FIG. 8. Vortex-glass transition line extracted from the following references: Hollow circles, (ceramic, dc transport) (Ref. 11). Black circles, (thin film, dc transport) (Ref. 12). Hollow triangles, (thin film, ac transport) (Ref. 13). Black triangles, (single crystal, dc transport) (Ref. 14). Hollow squares, (single crystal, ac transport) (Ref. 15). Black squares, this work. Black diamonds, $T_{\rm th}(B)$.

CONCLUSION

On the basis of a dynamical Brownian motion of vortices, we derive an expression of the current-voltage curves assuming a pinning well gradients distribution in a one-dimensional model which predicts Ohmic regimes in the limit of vanishing currents. The study of the distribution maxima reveal the existence of two dissipation mechanisms separated by a $T_{\rm th}(B)$ border line. Below $T_{\rm th}(B)$, the dissipation is governed by the current-induced force acting on vortices so the distribution describes the pinning relief and is temperature independent. Above $T_{\rm th}(B)$, thermal activation dominates and the extracted distributions become meaningless. This limits the validity of the model to regimes where collective effects can be neglected.

[1] P. W. Anderson, Phys. Rev. Lett. **9**, 309 (1962); P. W. Anderson and Y. B. Kim, Rev. Mod. Phys. **36**, 39 (1964).
[2] T. T. M. Palstra, B. Batlogg, L. F. Schneemeyer, and J. V. Waszczak, Phys. Rev. Lett. **61**, 1662 (1988); T. T. M. Palstra, B. Batlogg, R. B. Van Dover, L. F. Schneemeyer, and J. V. Waszczak, Appl. Phys. Lett. **54**, 763 (1989); Phys. Rev. B **41**, 6621 (1990).
[3] J. C. Soret, L. Ammor, B. Martinie, Ch. Goupil, V. Hardy, J. Provost, A. Ruyter, and Ch. Simon, Physica C **220**, 242 (1994).
[4] J. Bardeen and M. J. Stephen, Phys. Rev. A **140**, 1197 (1965).
[5] R. Griessen, Phys. Rev. Lett. **64**, 1674 (1990).
[6] M. Inui, P. B. Littlewood, and S. N. Coppersmith, Phys. Rev. Lett. **63**, 2421 (1989).
[7] B. Chen and J. Dong, Phys. Rev. B **44**, 10 206 (1991).
[8] M. Tinkham, *Introduction to Superconductivity* (McGraw-Hill, New York, 1975), Chap. 5.
[9] V. Ambegaokar and B. I. Halperin, Phys. Rev. Lett. **22**, 1364 (1969).
[10] H. A. Kramers, Physica **7**, 284 (1940).
[11] T. K. Worthington, E. Olsson, C. S. Nichols, T. M. Shaw, and D. R. Clarke, Phys. Rev. B **43**, 10 538 (1991).
[12] D. G. Xenikos, J. T. Kim, and R. Lemberger, Phys. Rev. B **48**, 7742 (1993).
[13] J. Deak, M. McElfresh, R. Muenchausen, S. Foltyn, and R. Dye, Phys. Rev. B **48**, 1337 (1993).
[14] N. C. Yeh, W. Jiang, D. S. Reed, U. Kriplani, and F. Holtzberg, Phys. Rev. B **47**, 6146 (1993).
[15] D. S. Reed, N. C. Yeh, W. Jiang, U. Kriplani, and F. Holtzberg, Phys. Rev. B **47**, 6150 (1993).
[16] M. P. A. Fisher, T. A. Tokuyasu, and A. P. Young, Phys. Rev. Lett. **66**, 2931 (1991).